Biophysical Journal Volume 86 June 2004 3855–3862

Extended Molecular Dynamics Simulation of the Carbon Monoxide Migration in Sperm Whale Myoglobin

Cecilia Bossa,* Massimiliano Anselmi,* Danilo Roccatano,† Andrea Amadei,‡ Beatrice Vallone,§ Maurizio Brunori,§ and Alfredo Di Nola*

*Department of Chemistry, University of Rome "La Sapienza", Rome, Italy; †Department of Chemistry, Chemical Engineering and Materials, University of L'Aquila, L'Aquila, Italy; ‡Department of Chemistry, University of Rome "Tor Vergata", Rome, Italy; and §Istituto Pasteur-Fondazione Cenci Bolognetti and Department of Biochemical Sciences "A. Rossi Fanelli", University of Rome "La Sapienza", Rome, Italy

ABSTRACT We report the results of an extended molecular dynamics simulation on the migration of photodissociated carbon monoxide in wild-type sperm whale myoglobin. Our results allow following one possible ligand migration dynamics from the distal pocket to the Xe1 cavity via a path involving the other xenon binding cavities and momentarily two additional packing defects along the pathway. Comparison with recent time resolved structural data obtained by Laue crystallography with subnanosecond to millisecond resolution shows a more than satisfactory agreement. In fact, according to time resolved crystallography, CO, after photolysis, can occupy the Xe1 and Xe4 cavities. However, no information on the trajectory of the ligand from the distal pocket to the Xe1 is available. Our results clearly show one possible path within the protein. In addition, although our data refer to a single trajectory, the local dynamics of the ligand in each cavity is sufficiently equilibrated to obtain local structural and thermodynamic information not accessible to crystallography. In particular, we show that the CO motion and the protein fluctuations are strictly correlated: free energy calculations of the migration between adjacent cavities show that the migration is not a simple diffusion but is kinetically or thermodynamically driven by the collective motions of the protein; conversely, the protein fluctuations are influenced by the ligand in such a way that the opening/closure of the passage between adjacent cavities is strictly correlated to the presence of CO in its proximity. The compatibility between time resolved crystallographic experiments and molecular dynamics simulations paves the way to a deeper understanding of the role of internal dynamics and packing defects in the control of ligand binding in heme proteins.

INTRODUCTION

The internal structure of proteins reveals the presence of a number of cavities of relatively small volume (<100 Å^3) that were identified early on (Richards, 1977) and have been repeatedly observed. Since these packing defects are associated with a reduction of thermodynamic stability, one may wonder why they were retained during evolution. Given that conformational mobility and internal dynamics are essential components of function and catalysis (Frauenfelder et al., 1988; Guo et al., 2001), it is often thought that discontinuities in internal packing of a protein help flexibility and thereby action at the physiological temperature for the particular organism. However, over the last few years a number of studies, largely carried out using myoglobin (Mb) as a model system, revealed that small cavities in the matrix of globular proteins may actually play a specific role in controlling function (see Brunori and Gibson, 2001; Schlichting and Chu, 2000; and references therein). This view of a possible functional role of internal packing defects came about as a result of several studies on the kinetics, spectroscopy, and crystallography of wild-type (wt) and mutant Mbs (Schlichting and Chu, 2000; Scott et al., 2001; and references therein). The work carried out by Scott and Gibson (1997) showed that xenon (which is known to bind to Mb at four specific sites called Xe1–Xe4; Tilton et al., 1984) controls the rate of ligand recombination after photolysis of liganded Mb and inspired several other investigations including recent time resolved Laue crystallographic experiments carried out at the European Synchrotron Radiation Facility (Grenoble, France) with subnanosecond to millisecond time resolution (Srajer et al., 1996, 2001; Schotte et al., 2003; Bourgeois et al., 2003). The very recent articles by Schotte et al. (2003) and Bourgeois et al. (2003) on mutants of Mb extended the pioneering work by Moffat and coworkers (Srajer et al., 1996, 2001). These new results revealed the time dependence of a number of structural changes involving the heme, the amino acid residues coating the distal heme pocket, the helices E and F, and the FG corner; noteworthily, the conformational dynamics of the globin structure was shown (Bourgeois et al., 2003) for the first time to follow an extended time course, providing a structural interpretation of the relaxation between conformational substates (Austin et al., 1975; Hagen and Eaton, 1996). Moreover the migration of CO (liberated inside the protein by laser photolysis of crystalline MbCO) was followed directly by x-ray diffraction and was shown in

Submitted November 20, 2003, and accepted for publication February 12, 2004.

Address reprint requests to Alfredo Di Nola, Dept. of Chemistry, University of Rome "La Sapienza", P.le Aldo Moro 5, 00185 Rome, Italy. Tel.: 39-06-4991-3122; Fax: 39-06-490324; E-mail: dinola@degas.chem.uniroma1.it.

Danilo Roccatano's present address is School of Engineering and Science, International University of Bremen, Bremen, Germany.

0006-3495/04/06/3855/08 $2.00

doi: 10.1529/biophysj.103.037432

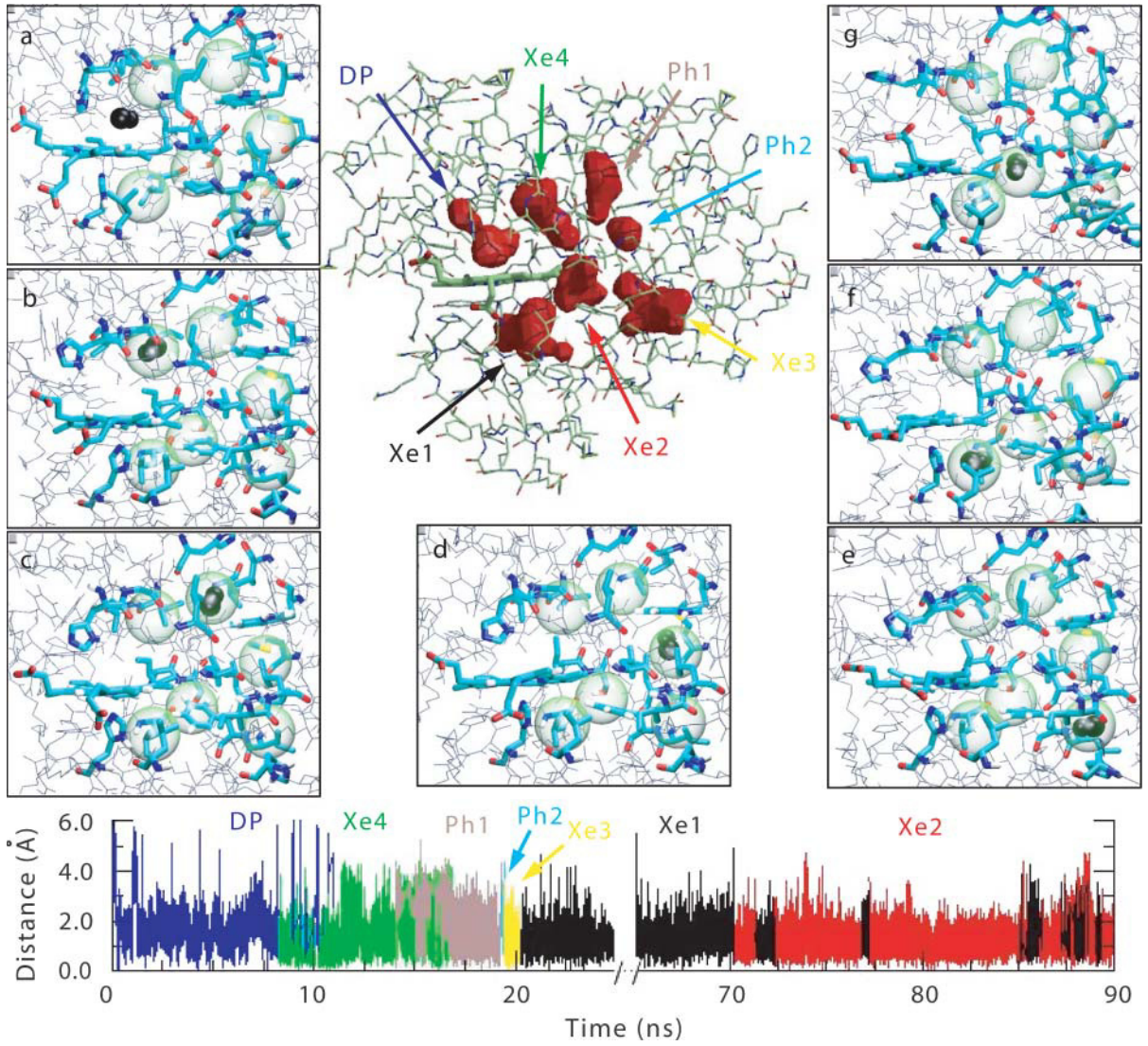

FIGURE 1 (*Top*) In the center we have reported the crystal structure of the wild-type CO-bound sperm whale Mb. The cavities involved in the migration of the ligand, detected by the package SURFNET (Laskowski, 1995), are shown in red and indicated by legends of different colors. CO is not shown. *a–g* illustrate different snapshots of the CO migration, as obtained by the MD simulation, showing the ligand (in *black*) in the DP, Xe4, Ph1, Ph2, Xe3, Xe1, and Xe2 cavities, respectively. For clarity sake, the cavities are represented by identical spheres but the DP is not highlighted. In *a*, the CO orientation parallel to the heme plane is to be noted; in *g*, the outward rotation of the His-(E7)64 side chain corresponds to an open His gate. (*Bottom*) The trajectory of the distance between the CO center of mass and the (arbitrarily chosen) center of each cavity is depicted. Consistently with the color code of the central panel, the lines represent the following location of CO: blue for DP, green for Xe4, brown for Ph1, cyan for Ph2, yellow for Xe3, black for Xe1, and red for Xe2. A few backward and forward transitions between adjacent cavities can be observed (DP–Xe4 at $t = 10$ ns; Xe4–Ph1 at $t = 15$ ns; Xe1–Xe2 in the range 70–90 ns); in the time range 25–65 ns (not shown), CO remains in the Xe1 cavity. It may be noticed that transitions in between cavities are very fast, showing that the ligand is rapidly hopping through channels connecting the cavities.

two different mutants to populate the Xe4 cavity on the distal side of the heme before populating the Xe1 cavity on the proximal side (Schotte et al., 2003; Bourgeois et al., 2003). Migration of CO around the heme occurred over the time span of several nanoseconds to microseconds, in agreement with the results of Srajer et al. (2001) on wt Mb.

Outstanding as they are, these crystallographic results can sample the 3D structure at selected times after photolysis, providing high resolution structural information on the relaxation of the globin moiety over a time range now accessible to molecular dynamics (MD) simulations. This article reports an extended (90 ns) MD simulation on the migration of photodissociated CO in wild-type sperm whale Mb. Our results allow following one of the possible ligand migrations from the distal pocket (DP) to the Xe1 cavity via a path involving sequentially the other Xe binding cavities and momentarily two additional packing defects along the pathway. Our data refer to a single trajectory, so that we have

TABLE 1 Cavity volume in the crystal, occurrence of each cavity in the 90-ns MD simulation (% of time), time of residence of CO in each cavity, and time interval of the CO residence

Cavity	Cavity volume in the crystal (Å^3)	Occurrence of the cavity (% of time)	Total time of residence (ns)	Time interval (ns)
DP	67.1	92.7	8.6	0–10.9
Xe1	76.3	98.6	53.0	20.2–89.3
Xe2	44.5	70	16.8	70.2–89.9
Xe3	94.7	62.9	0.7	19.5–20.2
Xe4	67.6	26.6	7.5	8.2–16.8
Ph1	60.4	98	3.2	11.7–19.3
Ph2	18.4	33.5	0.1	16.5–19.4

no information on the overall kinetics. However, the local dynamics of the ligand in each cavity is sufficiently equilibrated to obtain local structural and thermodynamic information. Free energy calculations of the ligand migration between adjacent cavities clearly show that migration of the ligand is not a simple diffusion, but it is kinetically or thermodynamically driven by the collective motions of the protein. Conversely, we show that the protein fluctuations are influenced by the ligand in such a way that the opening/closure of the passage between adjacent cavities is strictly correlated to the presence of CO in its proximity. A number of local conformational changes at the heme, the iron, and a few selected residues are in satisfactory agreement with the crystallographic data. Thus for the first time, to our knowledge, it is possible to compare the overall relaxation of Mb as obtained by experiment with the simulation behavior from picoseconds to 90 ns and to draw valuable considerations not accessible to experimental techniques. This paves the way to a detailed description of the structural dynamics of a protein and its energy landscape, known to be so crucial to the control of function and folding (Frauenfelder et al., 1991; Dinner et al., 2000).

METHODS

Initial coordinates for the simulation of Mb with photodissociated CO were taken from the 1.15-Å resolution crystal structure of the CO-bound sperm whale Mb (PDB entry 1BZR) (Kachalova et al., 1999), in which we cut the CO–Fe bond. Thus from the beginning of the simulation the system was modeled as an unliganded state of Mb with CO.

MD simulations were performed with the Gromacs software package (Berendsen et al., 1995) using a modified GROMOS96 force field (van Gunsteren et al., 1996). The CO molecule was modeled with the three-site ''quadrupolar'' CO model of Straub and Karplus (1991). Simulations were carried out at constant temperature of 300 K within a fixed-volume rectangular box using periodic boundary conditions. The Lincs algorithm (Hess et al., 1997) to constrain bond lengths and the rototranslational constraint algorithm (Amadei et al., 2000) were used. The system, simulated in the presence of explicit simple point charge water molecules (Berendsen et al., 1981), contained ~5500 H_2O and a total of ~18,500 atoms. The initial velocities were taken randomly from a Maxwellian distribution at 300 K. By using dummy hydrogen atoms (Feenstra et al., 1999), a time step of 4 fs could be chosen; as suggested by Feenstra et al. (1999), we have redistributed the water oxygen mass on the hydrogen atoms to improve the stability of the simulation. A nonbond pair list cutoff of 9.0 Å was used and the pair list was updated every four time steps. The long-range electrostatic interactions were treated with the particle mesh Ewald method (PME) (Essman et al., 1995) using a grid size of 48 × 56 × 54 (grid spacing of 0.12 nm) combined with a fourth-order B-spline interpolation to compute the potential and forces in between grid points.

The solvent was relaxed by energy minimization followed by 50 ps MD at 300 K, while restraining protein atomic positions with a harmonic potential. The system was then minimized without restraints and its temperature brought to 300 K in a stepwise manner: 50-ps MD runs were carried out at 50, 100, 200, 250, and 300 K before starting the production runs at 300 K.

During the simulation, the temperature was held constant by the Berendsen algorithm (Berendsen et al., 1984). The protein and the rest of the system were coupled separately to the temperature bath.

The package SURFNET (Laskowski, 1995) was used for detecting the cavities and calculating their volume. In this program, gap regions are defined by filling the empty regions in the interior of the molecule with gap spheres of variable radius (Rmin = 1.0 Å and Rmax = 3.0 Å, in our case). These spheres are then used to compute a 3D density map that, when contoured, defines the surface of the gap region.

TABLE 2

	CO in DP (3–8 ns)	CO in Xe4–Xe3 (8–20 ns)	CO in Xe1 (20–70 ns)	CO in Xe1–Xe2 (70–90 ns)	Experimental values*
Heme shift C→A (Å)†	−0.11 (0.09)	0.11 (0.04)	0.23 (0.02)	0.16 (0.04)	0.19
Heme tilt B–D (°)‡	4.1 (0.9)	2.2 (0.5)	1.4 (0.3)	1.0 (0.5)	4
Fe–N_4 plane (Å)§	0.23 (0.07)	0.23 (0.07)	0.23 (0.07)	0.23 (0.07)	0.29
Tilt of pyrrole rings with respect to the N_4 plane (°)	A: 8.7 (1.5)	A: 4.0 (1.3)	A: 11.2 (0.5)	A: 7.4 (0.9)	A: 5.1
	B: 9.7 (1.6)	B: 3.7 (1.3)	B: 7.6 (0.5)	B: 0.5 (1.2)	B: 5.5
	C: 10.7 (1.5)	C: 6.8 (1.2)	C: 10.5 (0.5)	C: 9.1 (0.8)	C: 12.4
	D: 6.3 (1.6)	D: 6.3 (1.0)	D: 9.6 (0.5)	D: 3.5 (0.9)	D: 9.9
Leu-89 (Cβ) displacement (Å)¶	0.78 (0.33)	0.62 (0.30)	1.16 (0.57)	0.85 (0.33)	NA
His-93 (Nε)–N_4 plane (Å)	2.2 (0.1)	2.2 (0.1)	2.2 (0.1)	2.2 (0.1)	2.45

NA, not available. Rows 1–5: Comparison of some structural properties of the heme, Leu-(F4)89, and His-(F8)93 in the MD simulation with respect to the CO-Mb crystallographic structure (standard deviations in parenthesis). In the last column the comparison between the corresponding MbCO and deoxy-Mb crystal structure is reported. Row 6: Distance between His-(F8)93 and the center of geometry of the heme; the experimental value refers to the deoxy-Mb crystal structure.

*Srajer et al. (2001); Kachalova et al. (1999).

†Shift of the heme group in the direction CA of Fig. 2.

‡Tilt of the heme plane around the BD axis of Fig. 2.

§Shift of the iron toward the proximal pocket.

¶Shift of the Leu-89 with respect to the crystal structure.

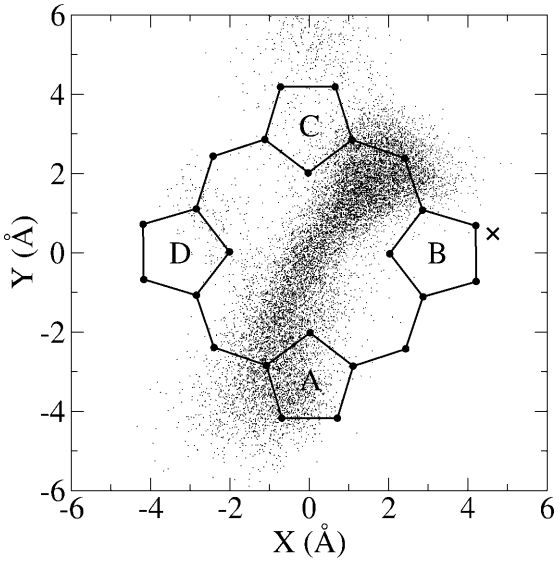

FIGURE 2 Projection of the CO center of mass onto the heme plane, as detected in the MD simulation. X indicates the projection of the Xe4 cavity.

We used essential dynamics technique (Amadei et al., 1993) to characterize the dynamical behavior of the protein and in particular to analyze in detail the principal components of some key residues motion.

The CO free energy calculations were performed using the potential of mean force (PMF) method (Beveridge and Di Capua, 1989).

RESULTS

Fig. 1 (*top central* structure) depicts the position and shape of the cavities in the crystal structure of MbCO as obtained by analysis performed with the package SURFNET (Laskowski, 1995). It can be noted that, in addition to the DP and Xe1–Xe4 cavities, two additional packing defects (hereafter called phantom 1 (Ph1) and phantom 2 (Ph2)) were detected. All these cavities (vide infra) play an important role for the CO migration inside the protein, acting as temporary docking sites. Table 1 reports the persistence of the cavities in the simulation, the time spent by CO in each cavity, and the corresponding time interval; it should be noted that all the cavities largely fluctuate during the MD simulation, with volume ranging from zero up to approximately twice their crystal value.

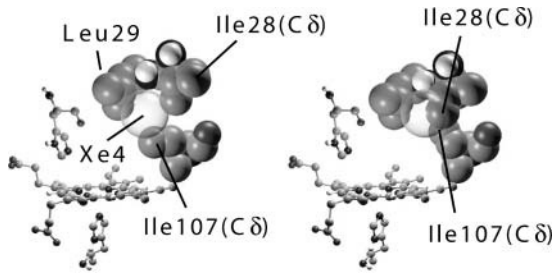

FIGURE 3 Representation of the hydrophobic cluster, formed by Ile-(B9)28, Leu-(B10)29, and Ile-(G8)107, that controls the opening (*left*) and closure (*right*) of the Xe4 cavity.

Snapshots of the CO migration within the protein, in the 90-ns MD simulation, are also reported in Fig. 1 (*a–g*). For the sake of clarity, the cavities are represented as identical spheres, without taking into account their actual dimensions and shapes. Table 1 reports the persistence of the cavities in the simulation and the percentage of residence time of CO in each one over the whole trajectory. The trajectory of the distances between the CO center of mass and the center of each cavity are reported in Fig. 1 (*bottom*). These data clearly show that during the simulation the ligand migrates from the DP to the Xe1 cavity, passing through Xe4, Ph1, Ph2, and Xe3, and then moving back into Xe2 for a while. Interestingly (Table 1; Fig. 1, *bottom*) the time of residence of CO in each cavity is different, most of the time being spent in DP, Xe4, Xe1, and Xe2.

Time resolved crystallographic data on wt Mb (Srajer et al., 2001) showed that photolyzed CO migrates from DP to Xe1 within less than 100 ns and stays there for many microseconds up toward milliseconds. Recent high resolution Laue diffraction results on two mutants of sperm whale Mb (Schotte et al., 2003; Bourgeois et al., 2003) show that CO occupies the Xe4 cavity before migrating to Xe1. The presence of CO in the other cavities was never observed, possibly due to the short time of residence. The path of CO within the protein is still unknown. It was hypothised a direct passage from the DP to the Xe2 and Xe1 cavities. Our results show, for the first time to our knowledge, one possible alternative path involving all the cavities. It has to be pointed out that the time of passage between adjacent cavities is almost instantaneous (Fig. 1 *bottom*), in agreement with previously reported calculations by Elber and Karplus (1990) that identified the photolyzed CO as hopping rapidly in between cavities. Moreover we observe 10 backward and forward passages from DP to Xe4 (Fig. 1 *bottom*, *blue* and *green* in the time range 8–11 ns), 20 from Xe4 to Ph1 (*green* and *brown* at 15 ns), and 15 from Xe1 to Xe2 (*black* and *red* in the time range 70–90 ns).

Time resolved crystallographic data on photolyzed wt (Srajer et al., 1996, 2001) and mutated Mbs (Schotte et al., 2003; Bourgeois et al., 2003) reported the time dependence of several structural changes seen by comparison with the static structures of MbCO and deoxy Mb. The shift and tilt of the heme in the photolysed Mb, the out-of-plane displacement of the iron atom toward the proximal His-(F8)93, and the motions of the distal residues and of the E and F helices are some of the prominent changes. They also described the displacement of Leu-(B10)29 and Leu-(F4)89, different CO locations in the DP and (as outlined above) the internal migration of photolyzed CO. We have monitored these features over the whole simulation.

Table 2 shows a comparison between experimental and simulated data. In particular the small changes in the heme orientation as well as the iron displacement (the latter being however mainly due to the force constant adopted to describe the iron–heme bond) are well reproduced. The His-(E7)64

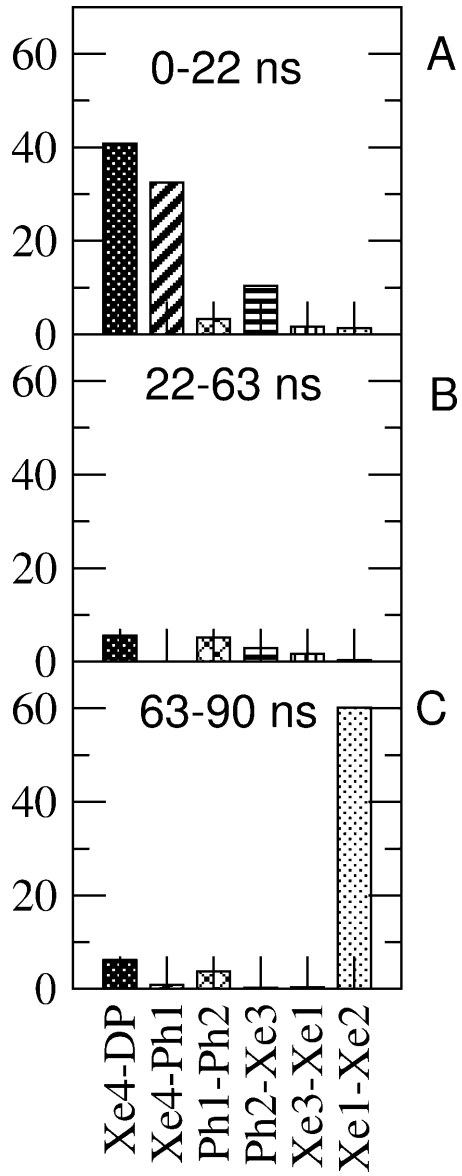

FIGURE 4 The bars report the fraction of time (in %) during which the connection between adjacent cavities remains open, expressed for the various channels over different time intervals (indicated).

behavior is notable, the χ_1 torsion angle distribution showing two well-defined populations (data not shown). One of these ($\chi_1 = -160°$) corresponds to the side chain oriented toward the heme, with a distance between the Nδ of His-(E7)64 and the center of geometry of the four pyrrole nitrogens of 5.5–6.0 Å. This distance is shorter than in the MbCO crystal and comparable to that measured in the deoxy Mb, in agreement with experimental evidence from time resolved crystallography (Srajer et al., 2001). The other χ_1 value ($-75°$) corresponds to a configuration that opens the so-called His gate, best seen in Fig. 1 *g* at ~80 ns. It is significant that the flipping between these two configurations of His-(E7)64 is present over the whole simulation.

The projection of the CO center of mass onto the heme plane (Fig. 2), as obtained in the MD simulation, clearly shows that CO populates a subspace connecting the pyrrole ring A to a region in between the B and C rings. It is interesting to note that the latter position is more densely populated and corresponds, almost exactly, to the one measured by low temperature (Schlichting et al., 1994; Teng et al., 1994; Hartman et al., 1996) and room temperature (Srajer et al., 2001) crystallography, and to the results of previously reported MD simulations (Meller and Elber, 1998; Vitkup et al., 1997; Ma et al., 1997); the other extreme location is very close to the position of His-(E7)64 in the crystal structure. The orientation of CO in the DP is largely parallel to the heme plane (see Fig. 1 *a*), with a preference for two opposite orientations, in excellent agreement with time resolved room temperature infrared spectroscopic measurements (Lim et al., 1995) and MD simulations (Meller and Elber, 1998).

The connection between the DP and the Xe4 cavity involves a hydrophobic cluster formed by Ile-(B9)28, Leu-(B10)29, and Ile-(G8)107. It was analyzed by an essential dynamics analysis, over the whole trajectory, of the three residues involved in the opening and closure of the DP–Xe4 connection. The results clearly show that the opening and closure of Xe4 cavity (Fig. 3) involves the motion of these residues, in particular the rotation of the χ_1 torsion angle of Ile-(B9)28 and of the χ_2 torsion angle of Ile-(G8)107, and the consequent upward motion of Leu-(B10)29. It is interesting to note that the probability of finding the connection between adjacent cavities open is greater when the ligand is in the cavities or nearby, whereas the probability is quite low when the ligand is far away (Fig. 4). Fig. 5 shows the trajectory of the Ile-(B9)28 χ_1 torsion angle during the simulation. It can be noted that the opening of the gate is significantly more frequent when the CO is in the proximity of the Ile-(B9)28.

This indicates that the protein dynamics is influenced by the nearby presence of the ligand. When the CO is in the Xe1 cavity, Leu-(F4)89 is displaced by ~1 Å with respect to its

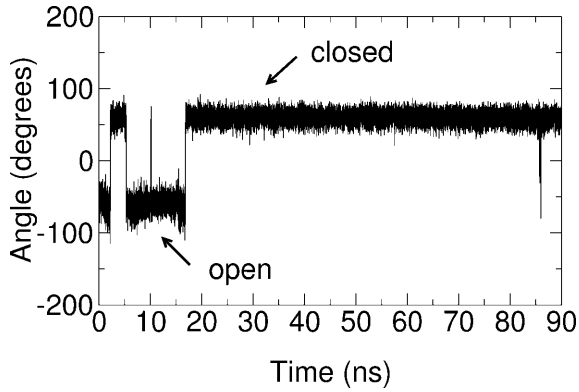

FIGURE 5 Trajectory of the Ile-(B9)28 χ_1 torsion angle during the simulation.

crystal structure position (Table 2), in agreement with experimental findings (Srajer et al., 2001). The migration from Xe1 to Xe2 cavity (see Fig. 1, *f* and *g*) is accomplished by the rotation of the Phe-(H14)138 side chain that opens the channel connecting the two cavities.

The MD simulation allows quantitatively analyzing the thermodynamics of the CO migration in the protein. We have calculated the free energy landscape of the CO by the use of the potential of mean force method (Beveridge and Di Capua, 1989). Briefly, the method is based on the choice of a direction and on the calculation of the mean force acting on the CO center of mass along this direction. The mean force corresponds to the free energy gradient. In Fig. 6, the mean force values (with their standard deviations) and the corresponding free energy landscapes are reported. The free energy plot shows that the free energy values of CO in the DP, Xe4, and Ph1 (Fig. 6 *A*) are comparable, differing in the two barriers and suggesting that migration could be kinetically controlled. Moreover, due to the different height of the barriers between DP–Xe4 and Xe4–Ph1, the probability of a backward migration is lower than the forward migration. Xe3–Xe1 and Xe1–Xe2 free energy plots (Fig. 6, *B* and *C*) show that the minima have almost the same value and are separated by a barrier of ~15 kJ/mol. For a better statistic, we have increased the sampling of the Xe3–Xe1 barrier crossing; as reported in the mean force plot the height of the free energy barrier is still not well determined. It has to be noted that, although the Xe3 cavity is exposed, the ligand does not escape from the Mb matrix because of the free energy barrier toward the solvent. Taken together these results show that the CO migration is not diffusive but is kinetically or thermodynamically driven by the collective motions of the protein.

CONCLUDING REMARKS

We have reported the results of a long (90 ns) MD simulation of wt Mb, revealing the relaxation dynamics of the

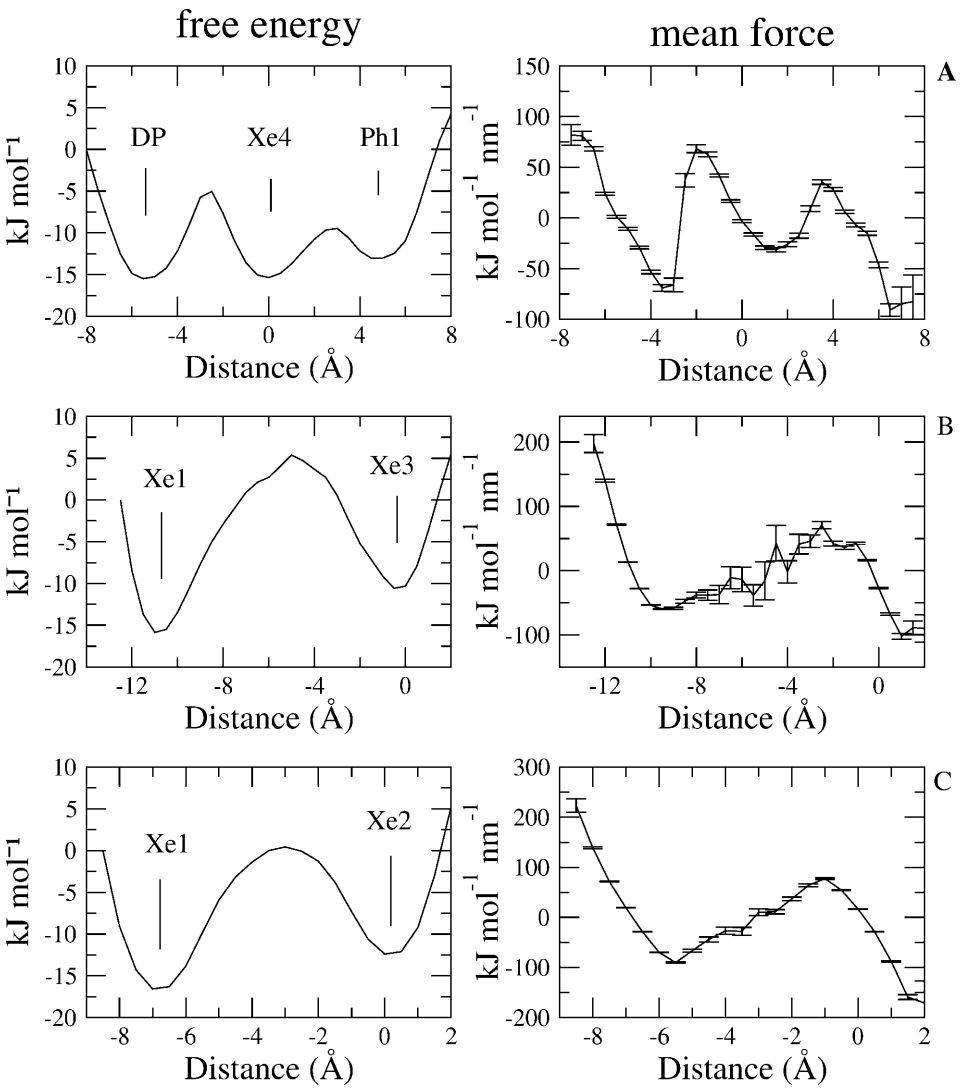

FIGURE 6 Mean forces (with their standard deviations) and CO free energy landscapes. (*A*) From DP to Ph1 cavity, the abscissa indicates the distance from the center of the Xe4 cavity. (*B*) From Xe3 to Xe1, the abscissa indicates the distance from the center of Xe3 cavity. (*C*) From Xe1 to Xe2, the abscissa indicates the distance from the center of Xe2 cavity.

hemeprotein after rupture of the Fe(II)–CO bond, which are compatible with the experimental data obtained by laser photolysis of MbCO. Comparison of our results with crystallographic data now available at high resolution on the transient states populated from 150 ps up to milliseconds (Schotte et al., 2003; Bourgeois et al., 2003) shows that over the range covered by the MD simulation the agreement with the experimental structural data is more than satisfactory. The tilt and shift of the heme, the out-of-plane motion of the iron, the conformational changes of several side chains (His-(E7)64, Leu-(B10)29, Leu-(F4)89, and others) are all reproduced almost quantitatively. This is an outstanding and positive result that is beneficial to both experiments and calculations. Moreover the progressive migration of the photolyzed CO from the distal pocket to the Xe1 cavity, as obtained by MD, is in agreement not only with time resolved room temperature crystallographic data (Srajer et al., 1996, 2001; Schotte et al., 2003; Bourgeois et al., 2003) but also with ultralow temperature spectroscopy and crystallography (Brunori and Gibson, 2001; Schlichting and Chu, 2000; Schlichting et al., 1994; Teng et al., 1994; Hartman et al., 1996).

Several MD studies of the CO dynamics in Mb were reported. Vitkup et al. (1997), Ma et al. (1997), and Meller and Elber (1998) have simulated the dynamics in the distal pocket with several short simulations in the picosecond range. In our simulation (Fig. 1 *bottom*,), CO spends ~8 ns in the DP, allowing a better statistics and sampling a conformational subspace of the protein not available in a shorter simulation. Overall, our results are in good agreement with the previous simulations in showing that CO in the DP, in addition to the position in between the B and C pyrrole rings, can populate a region close to the A ring (Fig. 2).

The CO migration within the protein has been extensively studied by MD simulations, in particular using the locally enhanced sampling algorithm proposed by Elber and Karplus (1990). Our results are in agreement with these authors who found that CO spends most of the time in the Xe cavities, and that transitions between cavities are rare and rapid events. Scott and Gibson (1997) showed for the first time that occupancy of these cavities by Xe has an effect on the ligand binding kinetics and thereby affects function. The presence of other cavities was also reported; Tilton et al. (1988) in a 96-ps simulation of the Mb-Xe complex showed that Xe can occupy transiently stable cavities not present in the original x-ray structure, and that it makes a few jumps between adjacent cavities.

As described in the previous section, our extended simulation allowed drawing a number of valuable considerations on the local structural dynamics of Mb that may not be accessible to crystallography, such as i), the dynamics of channel gating along the pathway between different cavities; ii), the role of the diatomic CO in forcing the way by pushing side chains; iii), the presence and significance of (previously unidentified) microcavities along the migration pathway; iv), the exact deformations of the heme (and thus possible computation of electronic transitions); v), the presence of alternative conformers of crucial residues, such as the distal His-(E7)64; and vi), finally a unique advantage of MD simulations is the possibility to calculate the free energy landscape that may provide direct information on CO migration kinetics inside the globin. These results clearly show that CO migration is not due to two different and uncorrelated random motions: the protein fluctuations and the random walk of the ligand. Instead these two motions are tightly coupled, as shown by the trajectory of the opening/closure of the gates between the cavities (Figs. 4 and 5), showing that the protein dynamics is influenced by the CO and by the free energy plots that show a nondiffusive character of the CO motion.

The comparison reported above, albeit more than satisfactory, is only a starting point given the fact that more trajectories are necessary to study the overall kinetics, and the role of crucial mutations should be explored. Nevertheless these data widen considerably the general significance of the successful experimental work by time resolved crystallography (Srajer et al., 1996, 2001; Schotte et al., 2003; Bourgeois et al., 2003) that is only accessible to a few model proteins such as Mb, given the technical need for synchronous trigger of the reaction in the crystal (as may be achieved by laser photolysis). Finally the physical connectivity of the packing defects in the protein matrix seen by crystallography and simulation consolidates the proposal of a novel significance and a functional role of the web of internal cavities in controlling ligand binding and some complex chemistry carried out by Mb (Brunori and Gibson, 2001; Brunori, 2001). The high resolution quantitative description of the structural dynamics of proteins from picoseconds to milliseconds will bring more insight crucial to our understanding of biochemistry and physiology.

This work was supported by grants from Ministero dell'Istruzione, dell' Università e della Ricerca (Progetto di Ricerca di Rilevante Interesse Nazionale 2003 on ''Structure and dynamics of redox protein'' to A.D.N. and M.B.) and from ''Centro di eccellenza in Biologia e Medicina Molecolare'' of the University of Rome ''La Sapienza''.

REFERENCES

Amadei, A., G. Chillemi, M. A. Ceruso, A. Grottesi, and A. Di Nola. 2000. Molecular dynamics simulations with constrained roto-translational motions: theoretical basis and statistical mechanical consistency. *J. Chem. Phys.* 112:9–23.

Amadei, A., A. B. Linssen, and H. J. C. Berendsen. 1993. Essential dynamics of proteins. *Proteins.* 17:412–425.

Austin, R. H., K. W. Beeson, L. Einsenstein, H. Frauenfelder, and I. C. Gunsalus. 1975. Dynamics of ligand binding to myoglobin. *Biochemistry.* 14:5355–5373.

Berendsen, H. J. C., J. P. M. Postma, W. F. van Gunsteren, A. Di Nola, and J. R. Haak. 1984. Molecular dynamics with coupling to an external bath. *J. Chem. Phys.* 81:3684–3690.

Berendsen, H. J. C., J. P. M. Postma, W. F. van Gunsteren, and J. Hermans. 1981. Interaction models for water in relation to protein hydration. *In* Intermolecular Forces. B. Pullman, editor. D. Reidel Publishing Company, Dordrecht, The Netherlands. 331–342.

Berendsen, H. J. C., D. van der Spoel, and R. van Drunen. 1995. GROMACS: a message-passing parallel molecular dynamics implementation. *Comp. Phys. Comm.* 95:43–56.

Beveridge, D. L., and F. M. Di Capua.1989. Free energy via molecular simulation: a primer. *In* Computer Simulation of Biomolecular Systems. W. F. van Gunsteren and P. K. Weiner, editors. ESCOM, Leiden. 1–26.

Bourgeois, D., B. Vallone, F. Schotte, A. Arcovito, A. E. Miele, G. Sciara, M. Wulff, P. Anfinrud, and M. Brunori. 2003. Complex landscape of protein structural dynamics unveiled by nanosecond Laue crystallography. *Proc. Natl. Acad. Sci. USA.* 100:8704–8709.

Brunori, M. 2001. Nitric oxide moves myoglobin centre stage. *Trends Biochem. Sci.* 26:209–210.

Brunori, M., and Q. H. Gibson. 2001. Cavities and packing defects in the structural dynamics of myoglobin. *EMBO Rep.* 2:674–679.

Dinner, A. R., A. Sali, L. J. Smith, C. M. Dobson, and M. Karplus. 2000. Understanding protein folding via free-energy surfaces from theory and experiment. *Trends Biochem. Sci.* 25:331–339.

Elber, R., and M. Karplus. 1990. Enhanced sampling in molecular dynamics: use of the time-dependent Hartree approximation for a simulation of carbon monoxide diffusion through myoglobin. *J. Am. Chem. Soc.* 112:9161–9175.

Essman, V., L. Perera, M. L. Berkowitz, T. Darden, H. Lee, and L. G. Pedersen. 1995. A smooth particle mesh Ewald method. *J. Chem. Phys.* 103:8577–8593.

Feenstra, K. A., B. Hess, and H. J. C. Berendsen. 1999. Improving efficiency of large time-scale molecular dynamics simulations of hydrogen-rich systems. *J. Comput. Chem.* 20:786–798.

Frauenfelder, H., F. Parak, and R. D. Young. 1988. Conformational substates in proteins. *Annu. Rev. Biophys. Biophys. Chem.* 17:451–479.

Frauenfelder, H., S. G. Sligar, and P. G. Wolynes. 1991. The energy landscapes and motions of proteins. *Science.* 254:1598–1603.

Guo, H., Q. Cui, W. N. Lipscomb, and M. Karplus. 2001. Substrate conformational transitions in the active site of chorismate mutase. *Proc. Natl. Acad. Sci. USA.* 98:9032–9037.

Hagen, S. J., and W. A. Eaton. 1996. Non-exponential structural relaxations in proteins. *J. Chem. Phys.* 104:3395–3398.

Hartman, H., S. Zinser, P. Komnions, R. T. Schneider, G. U. Nienhaus, and F. Parak. 1996. X-ray structure determination of a metastable state of carbonmonoxy myoglobin after photodissociation. *Proc. Natl. Acad. Sci. USA.* 93:7013–7016.

Hess, B., H. Bekker, H. J. C. Berendsen, and J. G. E. M. Fraaije. 1997. LINCS: a linear constraint solver for molecular simulations. *J. Comput. Chem.* 18:1463–1472.

Kachalova, G. S., A. N. Popov, and H. D. Bartunik. 1999. A steric mechanism for inhibition of CO binding to heme proteins. *Science.* 284:473–476.

Laskowski, R. A. 1995. SURFNET: a program for visualizing molecular surfaces, cavities and intermolecular interactions. *J. Mol. Graph.* 13: 323–330.

Lim, M. H., T. A. Jackson, and P. A. Anfinrud. 1995. Mid-infrared vibrational spectrum of CO after photodissociation from heme: evidence for a ligand docking site in the heme pocket of hemoglobin and myoglobin. *J. Chem. Phys.* 102:4355–4366.

Ma, J., S. Huo, and J. E. Straub. 1997. Molecular dynamics simulation study of the B-states of solvated carbon monoxymyoglobin. *J. Am. Chem. Soc.* 119:2541–2551.

Meller, J., and R. Elber. 1998. Computer simulations of carbon monoxide photodissociation in myoglobin: structural interpretation of the B states. *Biophys. J.* 74:789–802.

Richards, F. M. 1977. Areas, volumes, packing, and protein structures. *Annu. Rev. Biophys. Bioeng.* 6:151–176.

Schlichting, I., J. Berendzen, G. N. Phillips, and R. M. Sweet. 1994. Crystal structure of photolysed carbonmonoxy-myoglobin. *Nature.* 371:808–812.

Schlichting, I., and K. Chu. 2000. Trapping intermediates in the crystal: ligand binding to myoglobin. *Curr. Opin. Struct. Biol.* 10:744–752.

Schotte, F., M. Lim, T. A. Jackson, A. V. Smirnov, J. Soman, J. S. Olson, G. N. Phillips, Jr., M. Wulff, and P. A. Anfinrud. 2003. Watching a protein as it functions with 150-ps time-resolved x-ray crystallography. *Science.* 300:1944–1947.

Scott, E. E., and Q. H. Gibson. 1997. Ligand migration in sperm whale myoglobin. *Biochemistry.* 36:11909–11917.

Scott, E. E., Q. H. Gibson, and J. S. Olson. 2001. Mapping pathways for O2 entry and exit from myoglobin. *J. Biol. Chem.* 276:5177–5188.

Srajer, V., Z. Ren, T.-Y. Teng, M. Schmidt, T. Ursby, D. Bourgeois, C. Pradervand, W. Schildkamp, M. Wulff, and K. Moffat. 2001. Protein conformational relaxation and ligand migration in myoglobin: a nanosecond to millisecond molecular movie from time-resolved Laue X-ray diffraction. *Biochemistry.* 40:13802–13815.

Srajer, V., T. Y. Teng, T. Ursby, C. Pradervand, Z. Ren, S. Adachi, W. Schildkamp, D. Bourgeois, M. Wulff, and K. Moffat. 1996. Photolysis of the carbon monoxide complex of myoglobin: nanosecond time-resolved crystallography. *Science.* 274:1726–1729.

Straub, J. E., and M. Karplus. 1991. Molecular dynamics study of the photodissociation of carbon monoxide from myoglobin: ligand dynamics in the first 10 ps. *Chem. Phys.* 158:221–224.

Teng, T. Y., V. Srajer, and K. Moffat. 1994. Photolysis-induced structural changes in single crystals of carbonmonoxy myoglobin at 40 K. *Nat. Struct. Biol.* 1:701–705.

Tilton, R. F., Jr., I. D. Kuntz, Jr., and G. A. Petsko. 1984. Cavities in proteins: structure of a metmyoglobin-xenon complex solved to 1.9 A. *Biochemistry.* 23:2849–2857.

Tilton, R. F., Jr., U. C. Singh, I. D. Kuntz, Jr., and P. A. Kollman. 1988. Protein-ligand dynamics. A 96 picosecond simulation of a myoglobin-xenon complex. *J. Mol. Biol.* 199:195–211.

van Gunsteren, W. F., S. Billeter, A. Eising, P. Hunenberger, P. Kruger, A. E. Mark, W. Scott, and I. Tironi. 1996. Biomolecular Simulations: The GROMOS96 Manual and User Guide. BIOMOS bv, Zurich, Groningen.

Vitkup, D., G. A. Petsko, and M. Karplus. 1997. A comparison between molecular dynamics and X-ray results for dissociated CO in myoglobin. *Nat. Struct. Biol.* 4:202–208.